Conformal mapping-based 3D face recognition

Przemyslaw Szeptycki, Mohsen Ardabilian, Liming Chen
MI Department, LIRIS Laboratory, Ecole Centrale de Lyon, 69134 Lyon, France
{przemyslaw.szeptycki, mohsen.ardabilian, liming.chen}@ec-lyon.fr

Wei Zeng, Davig Gu, Dimitris Samaras
Computer Science Department, Stony Brook University, Stony Brook NY 11790, USA
{zengwei, gu, samaras}@cs.sunysb.edu

Abstract

In this paper we present a conformal mapping-based approach for 3D face recognition. The proposed approach makes use of conformal UV parameterization for mapping purpose and Shape Index decomposition for similarity measurement. Indeed, according to conformal geometry theory, each 3D surface with disk topology can be mapped onto a 2D domain through a global optimization, resulting in a diffeomorphism, i.e., one-to-one and onto. This allows us to reduce the 3D surface matching problem to a 2D image matching one by comparing the corresponding 2D conformal geometric maps. To deal with facial expressions, the Möbius transformation of UV conformal space has been used to 'compress' face mimic region. Rasterized images are used as an input for $(2D)^2PCA$ recognition algorithm. Experimented on 62 subjects randomly selected from the FRGC dataset v2 which includes different facial expressions, the proposed method displays a 86.43%, 97.65% and 69.38 rank-one recognition rate in respectively Neutral vs. All, Neutral vs. Neutral and Neutral vs. Expression scenarios.

1. Introduction

Face is potentially the best biometrics for people identification related applications for its non instructiveness, contactless and socially well acceptance. Unfortunately, face recognition in 2D proves to be a very challenging task as intra-class variations, dues to factors as diverse as pose, lighting conditions, facial expressions, etc., are often much greater than inter-class variations [12]. The last years have witnessed 3D face models as a potential solution to deal with the two unsolved problems in 2D face recognition, namely lightning conditions and pose variations [1], thereby improving the effectiveness of face recognition systems. While 3D face models are theoretically insensible to lighting condition changes, they still require to be pose normalized before 3D facial shape-based matching. Moreover, as 3D face models describe 3D facial shapes, they are also more sensible to facial expression changes as compared to their 2D counterpart. As 3D facial shape matching is rather hard, several works in the literature propose to map 3D face models into some low-dimensional space, including the local isometric facial representation [2], the annotated facial model (AFM) [6], or conformal mapping [9]. In [9], Wang et al. proposed conformal parameterization to reduce surface matching complexity; they studied a family of conformal geometric maps for recognition purpose. The recognition algorithm was tested on a small data set containing 100 face scans from 10 subjects and achieved 98.4% rank one recognition rate using texture and shape maps.

In this paper, we propose to deepen this conformal mapping-based approach for 3D face recognition. The proposed approach makes use of conformal UV parameterization for mapping purpose and Shape Index decomposition for similarity measurement. The 3D facial surface matching problem is reduced to 2D image matching thanks to the resulted 2D conformal geometric maps. To deal with facial expressions, the Möbius transformation of UV conformal space is also used to 'compress' face mimic region. Rasterized images are used as an input for $(2D)^2PCA$ recognition algorithm. Experimented on 62 subjects randomly selected from the FRGC dataset v2 which includes different facial expressions, the proposed method displays a 86.43%, 97.65% and 69.38 rank-one recognition rate in respectively Neutral vs. All, Neutral vs. Neutral and Neutral vs. Expression scenarios.

The remaining of this paper is organized as follows: section 2 gives brief introduction to conformal maps and the whole process overview. Section 3 describes in details the idea to create expression insensitive face maps, starting from preprocessing, face cut, conformal transformation and expression compression. Section 4 presents variation of standard PCA algorithm which has better accuracy. Finally section 5 presents test data set and achieved results and section 6 concludes approach and marks future directions.

2. Basics of conformal geometry and architecture overview

We introduce in this section first the basics of conformal geometry-based parameterization then describe the overview of our approach.

2.1. Conformal UV parameterization for face normalization

It can be proven that there exists a mapping from any surface with a disk topology to a 2D unit disk [5], which is one-to-one, onto, and angle preserving. This mapping is called conformal mapping and keeps the line element unchanged, except for a local scaling factor[4]. Conformal maps have many appealing properties: (1) If the parameterization is conformal, then the surface is uniquely determined (up to a rigid motion) by the mean curvature with area stretching factor defined on the parameter domain. (2) Conformal parameterization depends on the geometry itself, not the triangulation of the surfaces. From a practical point of view, conformal parameterization is easy to control. Hence conformal parameterization is crucial for 3D shape matching and recognition. Consider the case of mapping a planar region S to the plane D.

Suppose S is a topological annulus, with boundaries $\partial S = \gamma_0$. γ_1 as shown in Figure 1. First, we compute a path γ_2 connecting γ_0 and γ_1. Then we compute a harmonic function $f : S \to R$, such that:

$$\begin{cases} f_{\gamma_0} &= 0 \\ f_{\gamma_1} &= 1. \\ \Delta f &= 0 \end{cases} \quad (1)$$

The level set of f is shown in Figure 1. Then ∇f is a harmonic 1-form.

We slice the surface along γ_2 to get a new surface $\tilde{S}$ with a single boundary. γ_2 become two boundary segments γ_2^+ and γ_2^- on $\tilde{S}$. Then we compute a function $g_0 : \tilde{S} \to R$, such that

$$\begin{cases} g_0|_{\gamma_2^+} &= 1 \\ g_0|_{\gamma_2^-} &= 0 \end{cases} \quad (2)$$

g_0 takes arbitrary value on other vertices. Therefore ∇g_0 is a closed 1-form defined on S. Then we find another function $g_1 : S \to R$, such that $\nabla g_0 + \nabla g_1$ is a harmonic 1-form $\nabla.(\nabla g_0 + \nabla g_1) = 0$.

Then we need to find a scalar λ, such that $*\nabla f = \lambda(\nabla g_0 + \nabla g_1)$, where $*$ is a the Hodge star operator

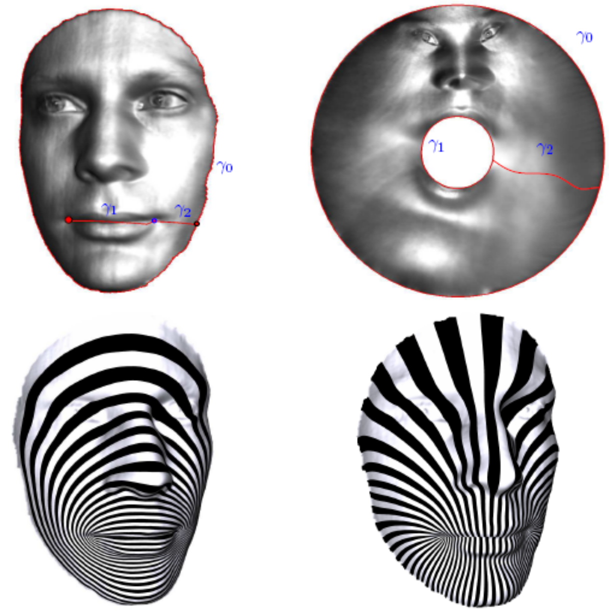

Figure 1. Harmonic 1-forms. Top row, the cut on the surface. Bottom row, the level sets of the harmonic 1-form ∇f and its conjugate harmonic 1-form $\lambda(\nabla g0 + \nabla g1)$.

($*(fdx + gdy) = fdy - gdx$, where $fdx + gdy$ is a differential one form). The holomorphic 1-form is given by

$$\omega = \nabla f + i\lambda(\nabla g_0 + \nabla g_1). \quad (3)$$

Let $Img(\int_{\gamma 0} \omega) = k$, the conformal mapping form S to a canonical annulus given by

$$\Phi(p) = exp^{\frac{2\Pi}{k} \int_q^p \omega}, \quad (4)$$

where q is the bas point, the path form q to p is arbitrary chosen.

For more details about conformal parameterization please refer to [9].

The result of conformal UV parameterization can be seen on Figure 2, where inner face hole created in lips part has been mapped to inner circle and outer 3D face boundary has been mapped to unit circle.

2.2. Process overview

The main idea underlying this approach is to transform a 3D facial shape matching problem to a 2D one using conformal parameterization. Furthermore, to deal with facial expression variations, we make use of Möbius transformation to 'compress' the elastic facial region, leading to a 2D conformal map less sensitive to facial expressions.

The overview of the whole pipeline to create conformal maps from 3D face models can be seen on Figure 3. Following sections will describe each step in details.

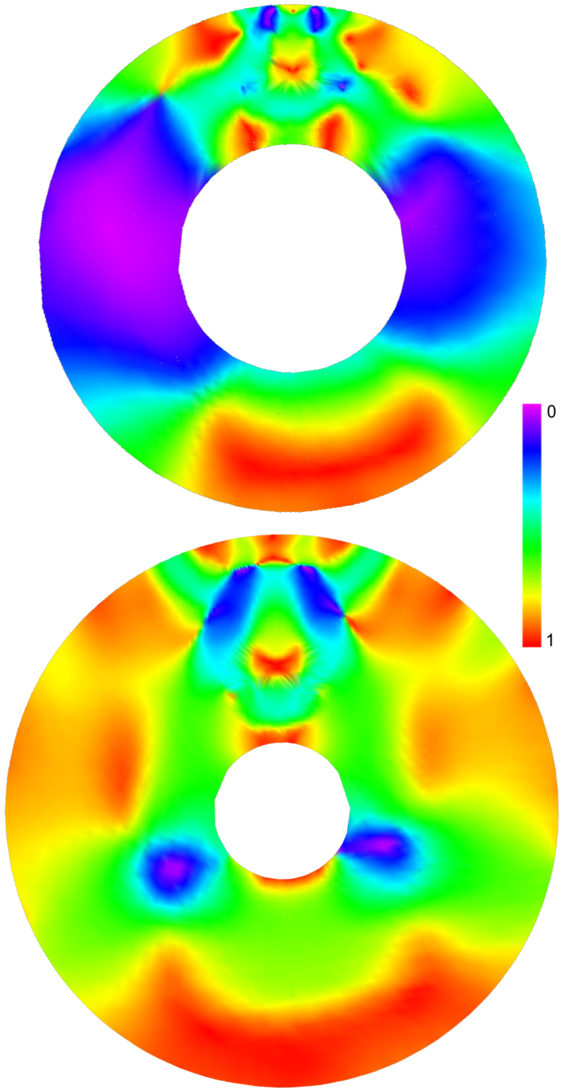

Figure 2. Conformal Map created from parametrized UV coordinates, colors represent Shape Index value. The mouth part has been mapped to the inner hole while outer face boundary to the boundary of circle (genus 0 surface, with a single boundary).

3. Generation of face conformal maps

3.1. 3D Face preprocessing

Direct application of conformal mapping introduced in [9] is not feasible on 3D face models as it requires surface with disk topology (genus 0 surface, with a single boundary). For this purpose, we have closed the mouth region based on manual landmarks [8], setting to zero the distance between the upper and the lower lips.

Conformal mapping is also sensitive to outer boundary [9]. To deal with this problem, faces are cropped using a fixed geodesic distance, 100 mm in this work, from the nose tip.

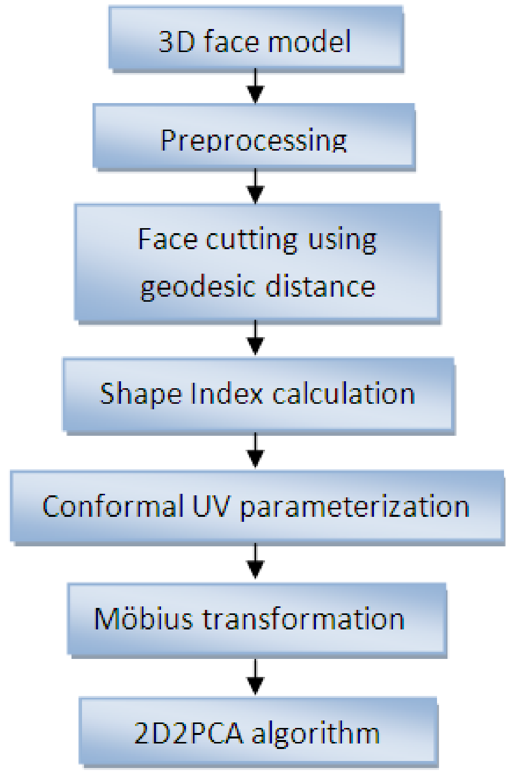

Figure 3. Following steps of the algorithm.

Once this preprocessing carried out, the 2D UV conformal parameterization of a 3D face model can be calculated according to [9]. Figure 4 shows the result of this preprocessing step. As we can see, closing the mouth while using geodesic distance for cropping 3D faces leads to a more consistent outer boundary, especially in the chin region, displaying roughly the same border the mouth being opened or closed.

3.2. Shape Index

Since UV conformal parameterization transfer 3D model to 2D map, some 3D property has to be moved over 2D face map. To deal with variations due to lightening conditions on texture images, we chose to project Shape Index values. Alternatively, we can also project other geometric measures such as normal vectors, curvatures, etc.

Shape Index (Figure 5) is a normalized curvature representation in a certain point of a surface within 2.5D image, proposed by Dorai and Jain in 1997. This local curvature information about a point is independent of the coordinate system. The Shape Index at point p is calculated using the maximum (k_1) and the minimum (k_2) local curvature:

Figure 4. Geodesic face cutting result with zero distance between lips in presence of expression.

$$SI(p) = \frac{1}{2} - \frac{1}{\pi} tan^{-1} \frac{k_1(p) + k_2(p)}{k_1(p) - k_2(p)}, \tag{5}$$

where k_1 and k_2 are principal curvatures at point p. This calculation process a shape scale between $< 0, 1 >$. Shape Index scale represents numerous shapes starting from a spherical cup (0 value) ending on spherical cap (1 value) (Figure 6).

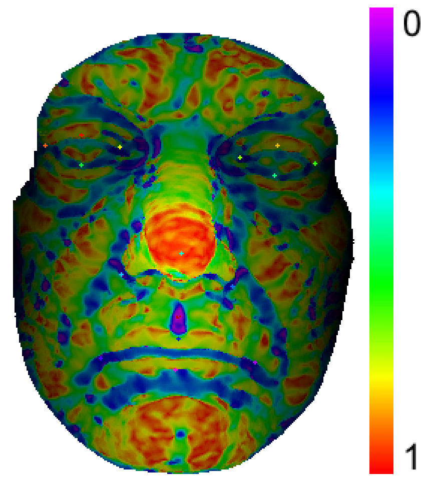

Figure 5. ShapeIndex decomposition over a face.

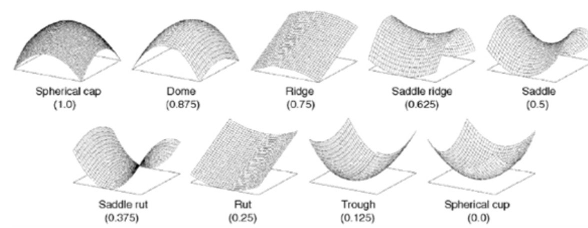

Figure 6. ShapeIndex - shape dictionary, possible shape index values and corresponding surface shape.

Shape Index is calculated using principal curvatures, whereas principal curvatures can be calculated as follows:

$$k_1(p) = H + \sqrt{H^2 - K}, \tag{6}$$

$$k_2(p) = H - \sqrt{H^2 - K}, \tag{7}$$

where, H and K are Mean and Gaussian curvatures in point p, which were calculated according to [8].

Curvatures of a vertex are computed by a least square fitting of a bi-polynomial surface onto an appropriate neighborhood around the vertex[8]. As can be seen on figure 5, too small neighborhood for estimating shape index leads to noisy decomposition. In this work, we used a neighborhood of 15 mm of geodesic distance from the vertex under investigation.

3.3. Conformal Map Normalization

Facial conformal maps generated by the harmonic energy minimization from 3D face models can have different size and 2D rotation. To facilitate matching 2D facial conformal maps, they need to be size and rotation normalized.

For rotation normalization we make use of the two inner eyes corners mapped on the conformal map then rotate the

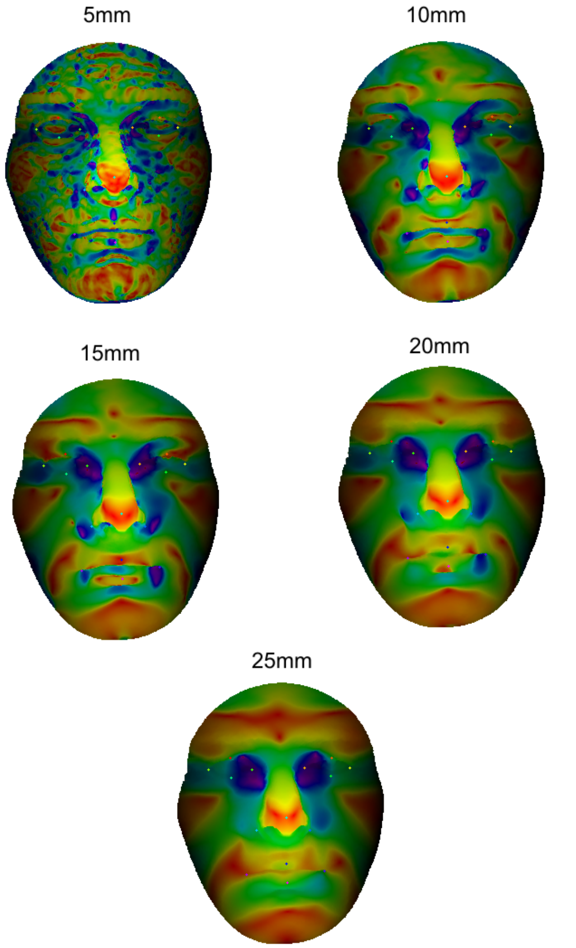

Figure 7. Difference in neighborhood in Shape Index approximation (neighborhood size indicated in mm, models marked with anchor points).

underlying conformal map so that both the two inner eye corners lie at the horizontal line. Once the pose corrected, the size of the underlying conformal map is also normalized, using the radius min-max rule, setting radius of conformal map to 50 units.

3.4. Compressing facial expression sensitive regions by Möbius transformation

Variations by facial expressions are a major challenge in 3D face recognition. Facial conformal maps so far generated have reduced a 3D shape matching problem to a 2D one while preserving facial topology. However, they are still facial expression sensitive. In order to decrease such a sensibility, we propose to make use of Möbius transformation to 'compress' facial elastic regions, i.e. the lower part of a face model. For this purpose, the center of a conformal map is moved to the nose tip of the face. Then Möbius transformation is carried out on UV conformal coordinates,

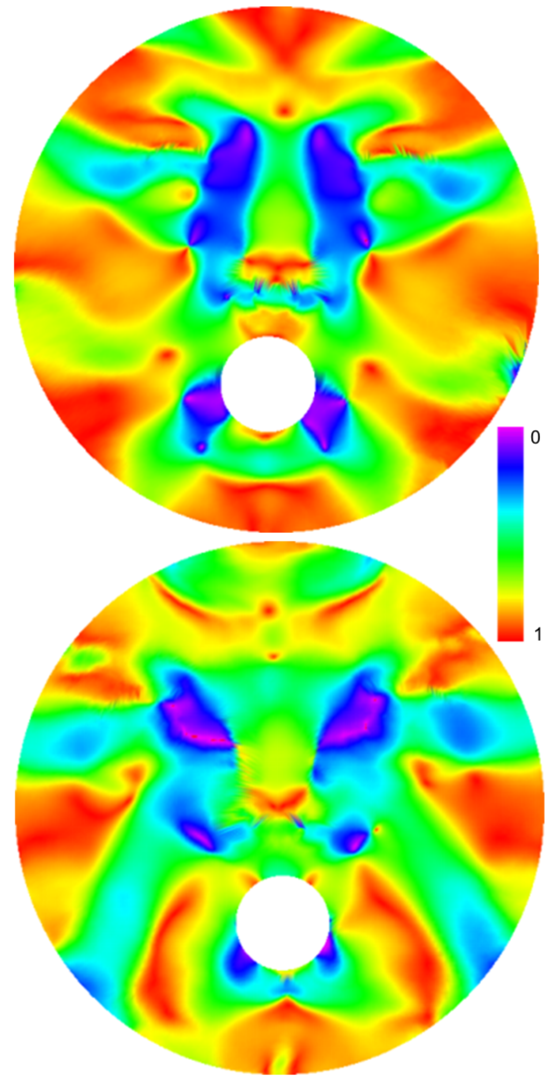

Figure 8. Conformal maps (Figure 2) transformed by Möbius transformation with center point in the nose tip.

using the following formula:

$$f(\theta, z_0, z) = e^{i\theta} \frac{z - z_0}{1 - \bar{z_0} z}, \tag{8}$$

where $z = (u + iv)$ is a complex number within the unit disk (UV coordinates). θ, z_0 and z are parameters. The mapping will move z_0 to the origin.

Figure 8 shows some results of this transformation on two facial conformal maps.

3.5. Conformal model rasterization - face map

Finally conformal maps resulted from Möbius mapping are rasterized. Rasterization is the process by which a primitive is converted to a two-dimensional image used for ex-

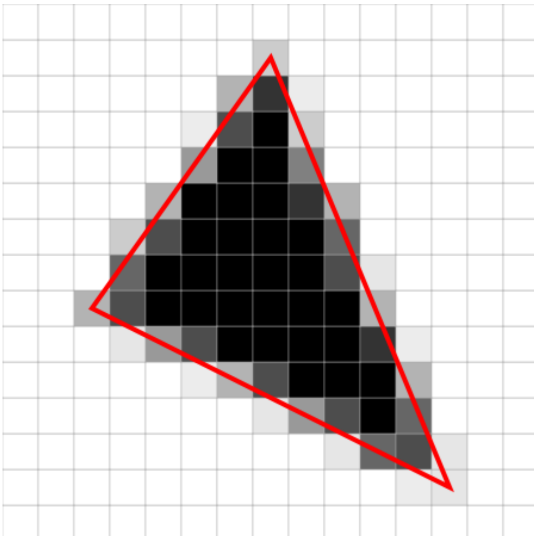

Figure 9. Example of single triangle rasterization (source Wikipedia).

ample to view 3D objects on the screen in 3D graphics. In our case such primitive is a triangle from which 3D model and then Conformal Map is formed. Figure 9 shows an example of one triangle rasterization.

The process consists of simple color interpolation between components of primitives; for our purpose we use simple version of rasterization which consists of triangle edge color interpolation and horizontal interpolation within edges.

4. $(2D)^2$PCA recognition algorithm

In this work $(2D)^2$PCA [3, 10], a variant of PCA with better performance, is used for feature dimension reduction and similarity computation.

Principal Component Analysis (PCA) is a well-known feature extraction and data representation technique however for 2D images it has one serious drawback, 2D image matrix have to be previously transformed to 1D vector by columns or rows concatenation. This type of concatenation into 1D vector often leads to a high-dimensional vector space, where it is difficult to evaluate covariance matrix accurately due to its large size and relatively small number of training samples [11, 10]. Also eigen decomposition of large covariance matrix is also very time-consuming.

To overcome those problems 2DPCA was proposed [10]. 2DPCA technique computes eigenvectors directly from so-called image covariance matrix, without conversion to 1D vector. 2DPCA is more efficient method than standard PCA having higher accuracy what was reported in [10].

As a standard 2DPCA method works in row directions, the alternative 2DPCA works in columns directions of images, $(2D)^2$PCA algorithm combines both of them [3]. In more details 2DPCA optimal matrix X reflecting information between rows of images, alternative 2DPCA learns optimal matrix Z reflecting informations between columns of images. $(2D)^2$PCA uses both matrixes X and Z to create coefficient (feature) matrix C:

$$C = Z^T AX, \tag{9}$$

As depicted in [10] the nearest neighbor classifier can be used for classification:

$$d(C, C_k) = \parallel C - C_k \parallel . \tag{10}$$

The method was tested on standard face image data base along with PCA and 2DPCA and gained higher accuracy with lower feature dimensionality. For more details of whole method please refer to [3].

5. Experimental results

5.1. Testing Data Set

To experiment our approach, 62 subjects were randomly selected from FRGCv2 data base [7]. FRGCv2 dataset contains 4007 3D scans of 466 persons. The data set were acquired using a Minolta910 range scanner with resolution of 640x480. Data set contains numerous subjects with different facial expressions, was collected during 2003-2004 academic year and hence includes the time variations. The data set contains also labeled expression variations like: NoExpression, Disgust, Happiness, Sadness, Surprise, Other.

5.2. Experimental Settings

For each 3D face model, the corresponding facial conformal map is generated using the whole process described above, including 3D face cropping, UV paramterization calculation, normalization, Möbius transformation and rasterization. The resulted 2D conformal maps were used as input for $(2D)^2$PCA algorithm for recognition, keeping 99% of eigenvalues variation.

One model with neutral expression from each selected subject is put to the gallery and the remaining models according to labeled expression are used as a probe in different scenarios: 1) Neutral vs. Neutral, 2) Neutral vs. Expression, 3) Neutral vs. All. In case of first scenario probe models are selected within "NoExpression" labels, in the second scenario probe models come from all models except those marked "NoExpression" and finally in the last scenario we take all expression and no-expression models as a testing probe.

5.3. Results and Analysis

Using this experimental setting, our approach has achieved 97.65% rank-one recognition rate for scenario

	I	II	III
ShapeIndex	86.43%	97.65%	69.38%
Mean Curv.	86.84%	94.29%	75.51%
Curvadness	86.23%	96.30%	70.91%
Kakadiaris 2007 PAMI[6]	97%	-	-
Wang 2006 CVPR[9]	95.7%	-	-

I - Neutral vs. All
II - Neutral vs. Neutral
III - Neutral vs. Expression

Table 1. Rank-1 recognition rate on 62 subjects of FRGCv2.0 data set.

where models labeled as "NoExpression" are presented to the system. All test scenarios and different combination of curvatures values are presented in Table 1.

For comparison reasons we have projected also different vertex features as a color maps. Shape Index is a normalized value in range $< 0, 1 >$ while mean curvature or cuvardness have no range, to create images with the same range, average maximum and minimum values were calculated using models form the Gallery.

As we can see in table 1 ShapeIndex Maps achieved best performance in the test Neutral vs. All (97.65%), but Cuvardness Index is not far away with result (96.3%). While in case of Expressions Mean curvature maps outperforms Shape Index maps with difference of 5%.

Comparing our approach to the previous article [9] we have achieved lower performance in the scenario of Neutral-All, but our algorithm has been tested on much bigger data set containing large expressions, while the tests made in the previous article were made only on 100 models without any mention about expressions. In [6] authors did not mention about recognition results in different scenarios and no results are provided to evaluate the sensibility of their algorithm with respect to expression variations. However, their technique requires first an ICP based accurate registration of 3D face scans.

6. Conclusion

In this paper we proposed to deepen the conformal geometry-based approach for face recognition in [9], using mouth as inner boundary and Möbius transformation to 'compress' facial expression sensitive regions. The major advantage of such an approach is to convert an initially 3D facial shape matching problem to a 2D one, thus making available all the techniques so far developed in 2D for 3D face recognition. Algorithm has been tested on FRGCv2 data base with different scenarios and achieved 86.43%, 97.65% and 69.38 rank-one recognition rate in respectively Neutral vs. All, Neutral vs. Neutral and Neutral vs. Expression scenarios.

The future work includes study of facial regions for conformal mapping and the use of other geometric measurements, such as curvatures, normal vectors, geometric images like also fusions of them.

7. Acknowledgment

This work was partially carried out within the French FAR3D project supported by ANR under the grant ANR-07-SESU-004 FAR3D.

References

[1] K. W. Bowyer, K. Chang, and P. Flynn. A survey of approaches and challenges in 3d and multi-modal 3d + 2d face recognition. *Computer Vision and Image Understanding*, 101(1):1–15, 2006. 1

[2] A. M. Bronstein, M. M. Bronstein, and R. Kimmel. Expression-invariant representations of faces. *IEEE Trans. PAMI*, 2004:1042–1053, 2007. 1

[3] L. Chen, G. Kukharev, and T. Ponikowski. The pca reconstruction based approach for extending facial image databases for face recognition systems. *Enhanced methods in computer security, biometric and artificial intelligence systems*, 2005. 6

[4] M. S. Floater and K. Hormann. Surface parameterization: a tutorial and survey. *Advances in multiresolution for geometric modelling*, pages 157–186, 2005. 2

[5] S. Haker, S. Angenent, A. Tannenbaum, R. Kikinis, G. Sapiro, and M. Halle. Conformal surface parameterization for texture mapping. *IEEE Transactions on Visualization and Computer Graphics*, 6(2):181–189, 2000. 2

[6] I. A. Kakadiaris, G. Passalis, G. Toderici, M. N. Murtuza, Y. Lu, N. Karampatziakis, and T. Theoharis. Three-dimensional face recognition in the presence of facial expressions: An annotated deformable model approach. *IEEE Transactions on Pattern Analysis and Machine Intelligence*, 29(4):640–649, 2007. 1, 7

[7] P. J. Phillips, P. J. Flynn, T. Scruggs, K. W. Bowyer, J. Chang, K. Hoffman, J. Marques, J. Min, and W. Worek. Overview of the face recognition grand challenge. *Computer Vision and Pattern Recognition*, 1:947–954, 2005. 6

[8] P. Szeptycki, M. Ardabilian, and L. Chen. A coarse-to-fine curvature analysis-based rotation invariant 3d face landmarking. *International Conference on Biometrics: Theory, Applications and Systems*, pages 1–6, 2009. 3, 4

[9] S. Wang, Y. Wang, M. Jin, X. Gu, and D. Samaras. 3d surface matching and recognition using conformal geometry. *IEEE Computer Society Conference on Computer Vision and Pattern Recognition*, pages 2453–2460, 2006. 1, 2, 3, 7

[10] J. Yang, D. Zhang, A. F. Frangi, and J. yu Yang. Two-dimensional pca: A new approach to appearance-based face representation and recognition. *IEEE Transactions on Pattern Analysis and Machine Intelligence*, 26(1'):131–137, 2004. 6

[11] D. Zhang and Z.-H. Zhou. (2d)2pca: 2-directional 2-dimensional pca for efficient face representation and recognition. *Neural Networks in Signal Processing*, 69:224231, 2005. 6

[12] W. Zhao, R. Chellappa, P. J. Phillips, and A. Rosenfeld. Face recognition: A literature survey. *ACM Comput. Surv.*, 35(4):399–458, 2003. 1